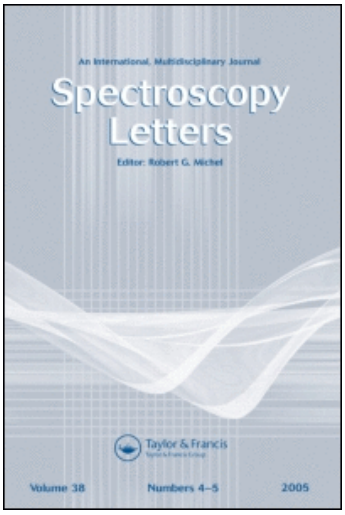

Spectroscopy Letters
Publication details, including instructions for authors and subscription information:
http://www.informaworld.com/smpp/title~content=t713597299

Nonlinear Luminescence Quenching in Eu_2O_3

Brian E. Trice[a]; Brian M. Tissue[a]
[a] Department of Chemistry, Virginia Polytechnic Institute and State University, Blacksburg, Virginia, USA

To cite this Article Trice, Brian E. and Tissue, Brian M.(2007) 'Nonlinear Luminescence Quenching in Eu_2O_3', Spectroscopy Letters, 40: 2, 333 — 348
To link to this Article: DOI: 10.1080/00387010701247597
URL: http://dx.doi.org/10.1080/00387010701247597

Spectroscopy Letters, 40: 333–348, 2007

ISSN 0038-7010 print/1532-2289 online
DOI: 10.1080/00387010701247597

Nonlinear Luminescence Quenching in Eu_2O_3

Brian E. Trice and Brian M. Tissue
Department of Chemistry, Virginia Polytechnic Institute and State University, Blacksburg, Virginia, USA

Abstract: We report a laser spectroscopic investigation of saturation effects in the spectra and dynamics of Eu_2O_3. The saturation effects occur at high laser intensity and appear as dips in the center of the fluorescence excitation lines and as a shortening of the $^5D_0$ excited-state decay curve. The saturation effects are observed in nanoparticles, micrometer-sized particles, and a fused crystal of monoclinic-phase Eu_2O_3 and in micrometer-sized particles of cubic-phase Eu_2O_3. We attribute the mechanism of the nonlinear luminescence quenching to upconversion by energy transfer.

Keywords: Energy transfer, europium oxide, intensity dependence, luminescence quenching, particle size dependence, upconversion

INTRODUCTION

Eu_2O_3 is a lanthanide oxide that is utilized for its luminescent and catalytic properties.[1,2] The close proximity of Eu^{3+} ions in Eu_2O_3 allows efficient energy transfer, and excitation energy can migrate to traps resulting in nonradiative quenching. This concentration quenching makes Eu_2O_3 too inefficient for use as a commercial phosphor, but it is commonly used as a source of Eu^{3+} ions in the production of doped phosphors, laser materials, and other

Received 19 June 2006, Accepted 11 July 2006
The authors were invited to contribute this paper to a special issue of the journal entitled "Spectroscopy of Lanthanide Materials." This special issue was organized by Professor Peter Tanner, City University of Hong Kong, Kowloon.
Address correspondence to Brian M. Tissue, Department of Chemistry (0212), Virginia Polytechnic Institute and State University, Blacksburg, VA 24061, USA. E-mail: tissue@vt.edu

technological materials. In addition to concentration quenching, high excitation density allows interactions between excited centers and additional nonradiative decay pathways such as cross-relaxation, also resulting in lower luminescence quantum efficiency. This nonlinear luminescence quenching has been documented in numerous systems including organic crystals, rare earth insulators, laser materials, semiconductors, and phosphors.

Much research has focused on determining the mechanisms of energy transfer and excited-state interactions in the solid phase.[3–5] An example is the development of quantum dot lasers.[6] Previous attempts to synthesize quantum dots that would lase were not successful due to Auger recombination. This excited-state interaction in semiconductors is identical to the process of upconversion by energy transfer in concentrated lanthanide systems. In both cases, the excited-state interactions result in a loss of excitation energy by a nonradiative pathway. Lasing in quantum dots requires a faster rate of stimulated emission than Auger recombination, which was accomplished by packing the quantum dots into a sufficiently small volume,[6] and more recently by optical engineering via nanocrystal shape and heterostructure formation.[7]

Understanding nonlinear luminescence quenching is also important for developing mathematical models of energy transfer. One general assumption in modeling is that the excited-state concentration is low enough that excited-state interactions do not occur. However, the excited-state concentration at which this assumption is valid depends on the system. Often, the influence of excited-state interactions on luminescence decay is ignored, which might explain why attempts to model energy migration in Eu_2O_3 have had limited success.[8] The difficulties were assumed to be due to the complex nature of the energy migration, which is a reasonable assumption because energy transfer in Eu_2O_3 is predicted to occur by multiple mechanisms.[8] However, nonlinear luminescence quenching due to excited-state interactions may also be a factor because energy transfer has been explained well in other concentrated systems.[9]

Bihari observed apparent saturation dips in the center of excitation lines during investigations into the spectra and dynamics of nano-sized monoclinic Eu_2O_3.[10] Trice replicated the saturation dips in cubic-phase Eu_2O_3 powder, and an example is shown in Figure 1. In this spectrum, the 580.7-nm line is the $^7F_0 \rightarrow {}^5D_0$ transition for Eu^{3+} in the C_2 crystallographic site, and the 582-nm line is a $^7F_1 \rightarrow {}^5D_0$ transition of Eu^{3+} in the S_6 crystallographic site. Although most saturation spectroscopy is observed in gas-phase samples, some interesting effects are reported recently for the condensed phase.[11,12] This paper presents a systematic investigation of the saturation effect observed in Eu_2O_3, specifically investigating the following possible mechanisms:

1. Instrumental artifacts.
2. Direct energy transfer to luminescence traps.
3. Two-photon absorption, excited-state absorption, and second harmonic generation.

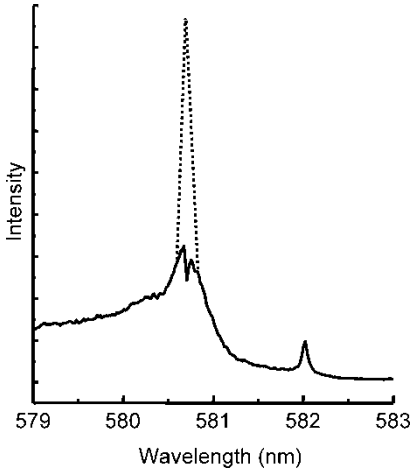

Figure 1. Fluorescence excitation spectrum of cubic-phase Eu_2O_3 powder (sample temperature $\sim$12 K, emission monitored at 612 nm). The dashed line shows the 579-nm excitation peak shape at lower laser intensity.

4. Superfluorescence, amplified spontaneous emission, and stimulated emission.
5. Localized heating.
6. Upconversion by energy transfer.

Most experiments to determine the mechanism of the saturation effect were done on micrometer-sized powders of cubic-phase Eu_2O_3. We also investigated the saturation effect as a function of sample type in monoclinic-phase Eu_2O_3, including nanoparticles, micrometer-sized powder, and a crystal.[13] By the process of elimination, we attribute the saturation to upconversion by energy transfer.

MATERIALS AND METHODS

Cubic-phase Eu_2O_3 powder (99.99%, Aldrich, Milwaukee, WI, USA) was sintered at 950°C in air overnight. Monoclinic-phase Eu_2O_3 samples were prepared from cubic-phase Eu_2O_3 powder by heating in a tube furnace to 1400°C in air for 4 h. The high temperature produces the metastable monoclinic form.[14,15] Nanoscale Eu_2O_3 particles were prepared by gas-phase condensation using a CO_2 laser to vaporize sintered pellets.[10,16] Vaporization took place in a N_2 buffer gas of 10–600 Torr, resulting in particles of 10–20 nm. During nanoparticle production, the Eu_2O_3 pellet is melted at the point of laser focus. On cooling, parts of the residual pellet remained as a pink, glassy-looking solid. A piece of this crystalline material, approximately 0.8 mm thick, was used to investigate the saturation effects in crystalline monoclinic Eu_2O_3.

The experimental methods included fluorescence excitation spectroscopy, fluorescence spectroscopy, and fluorescence transient measurements. All powdered samples were packed tightly into a 3-mm-diameter by 3-mm-deep depression in a copper sample holder. Large crystal samples were affixed to the sample holder with thermal grease. The sample holder was mounted to the cold head of a closed-cycle refrigerator (GB15, Cryomech, Syracuse, New York, USA), which maintained a sample temperature of approximately 12 K, and a heating unit on the cold finger allowed temperature-dependent studies up to 300 K.

The excitation source was a Nd^{3+}:YAG-pumped (Surelite II, Continuum, Santa Clara, CA, USA) tunable dye laser (ND60, Continuum, Santa Clara, CA, USA) operating at 10 Hz. Coumarin 540A laser dye (Exciton, Dayton, OH, USA) provided a scanning range of 516–590 nm with a linewidth of 0.03 nm ($\sim$1 cm^{-1}). The laser beam was focused onto the sample surface with a 6-cm focal length cylindrical lens. The line focus was more reproducible and lessened ablation of the powder out of the sample holder. The dye laser energy was adjustable between 2 to 400 μJ by adjusting the Nd^{3+}:YAG laser energy and by placing neutral-density filters in the dye laser beam. The excitation energy was monitored using a universal radiometer (Digirad R-752, Terahertz Technologies, Oriskany, NY, USA).

Site-specific excitation and fluorescence spectra were recorded with a 1-m monochromator (Spex 1000M, 0.08-nm spectral bandpass, HORIBA Jobin Yvon, Edison, NJ, USA) and a GaAs(Cs) photomultiplier tube (R636-10, Hamamatsu, Hamamatsu City, Japan). Excitation spectra monitoring broadband emission were recorded using a 0.25-m monochromator (Jarrell Ash, 6-nm bandpass, Genesis Laboratory Systems, Grand Junction, CO, USA) and an Sb-Cs photomultiplier tube (P28, Hamamatsu, Hamamatsu City, Japan). The output current of the photomultiplier tube was converted to a voltage signal using a 100-MHz bipolar amplifier (6931, Phillips Scientific, Mahwah, NJ, USA). This signal was processed and stored using a boxcar averager (SR250, Stanford Research Systems, Sunnyvale, CA, USA), an analog-to-digital data-acquisition board (Lab PC+, National Instruments, Austin, TX, USA), and a data acquisition program (LabView, National Instruments, Austin, TX, USA). Fluorescence transients were recorded by averaging at least 300 laser shots with a 350-MHz digital oscilloscope (TDS460, Tektronix, Richardson, TX, USA).

SATURATION MECHANISMS

Instrumental Artifacts

Before considering possible nonlinear quenching mechanisms, effects due to instrumental artifacts must be eliminated. Saturation at the maxima of excitation lines could appear due to saturation in the detector or electronics. That possibility was tested by placing neutral-density filters between the sample

and the monochromator to decrease the amount of radiation reaching the detector. The resulting excitation spectra (not shown) had a uniform signal decrease with no change in the relative depth of the dips. Another possible instrumental limitation to consider is an insufficient detector response time. This possibility was eliminated because it would be most severe at the leading edge of the time-resolved luminescence signal, and the saturation dip is greatest several microseconds after excitation. The holder geometry was approximately 45 degrees to the excitation beam and luminescence was collected at 90 degrees to the excitation beam. This geometry for the solid samples helps to minimize any prefilter saturation effects. Likewise, no self-absorption of the red luminescence is expected.

Direct Transfer to Traps

Energy transfer to traps can occur in Eu_2O_3 because of the high Eu^{3+} concentration. This trapping is referred to as concentration quenching and results in an overall decrease in luminescence output. If direct transfer to traps causes the saturation dips, the dips will not be dependent on the excitation density.[17] However, an excitation energy dependence study shown in Figure 2 shows that the excitation dips are intensity dependent. At low

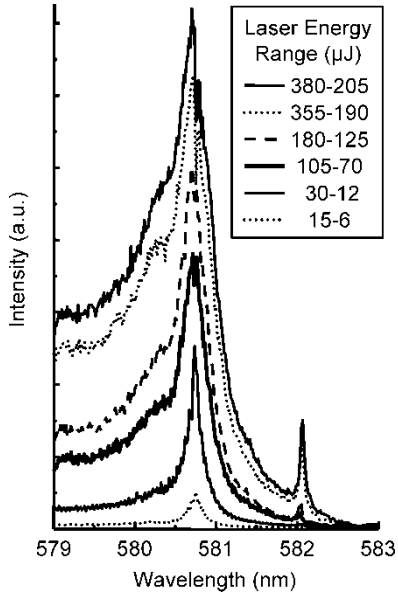

Figure 2. Fluorescence excitation spectra of cubic-phase Eu_2O_3 powder (sample temperature ~12 K, emission monitored at 612 nm). The laser energies are given for the start and end of the scan.

excitation density the dip is not present, and it only appears at excitation energies above 70 μJ. Thus the dip shows a direct dependence on excitation density and cannot be attributed to energy transfer to traps.

Multiple Photon Absorption

With instrumental artifacts and energy transfer to traps ruled out, the dips in the excitation spectra can only be explained in terms of a nonlinear relationship between excitation density and luminescence output. The first nonlinear process investigated was the multiple absorption of photons by individual Eu^{3+} ions. This process has been reported to occur in a number of luminescent systems including those doped with rare-earth ions.[18] The three possible mechanisms for multiple-photon absorption—two-photon absorption, second harmonic generation, and excited-state absorption—are illustrated in simplified energy diagrams in Figure 3. It is important to note that all three processes require a high excitation density and only occur during the laser excitation pulse.[19] Each of the multiple photon processes can potentially result in emission of anti-Stokes luminescence, although excitation to high-energy states in Eu_2O_3 is followed quickly by nonradiative decay to the $^5D_0$ excited state with no anti-Stokes luminescence.[20,21]

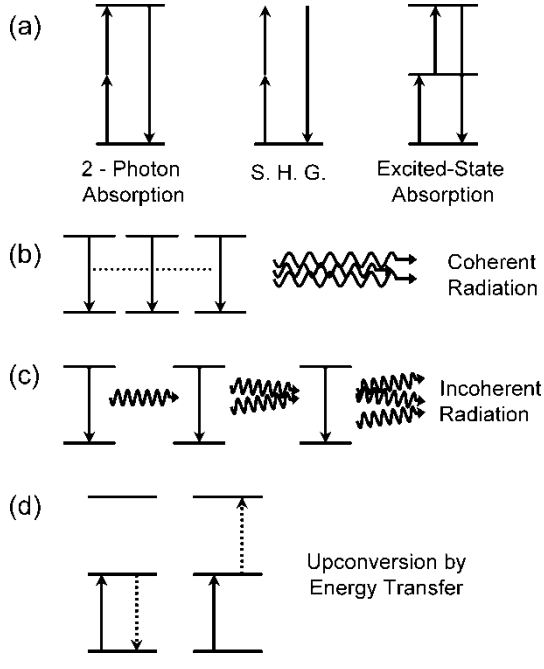

Figure 3. Energy level diagrams for (a) two-photon absorption processes, (b) superfluorescence, (c) amplified spontaneous emission, and (d) upconversion.

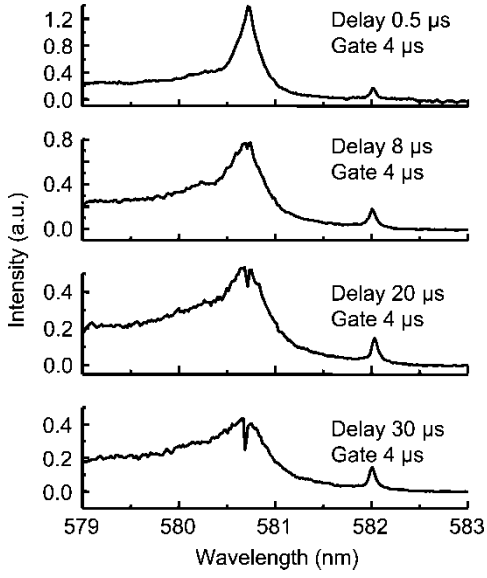

Figure 4. Fluorescence excitation spectra for cubic-phase Eu_2O_3 powder using various delay times (sample temperature ~12 K, emission monitored at 612 nm).

Multiple photon absorption was investigated by collecting excitation spectra of Eu_2O_3 using various delay times, as presented in Figure 4. The first excitation spectrum was collected using a boxcar delay of 0.5 μs and a gate of 4 μs. These experimental parameters selectively integrated the luminescence occurring immediately after excitation, and the spectrum showed no dip at the absorption maxima. The additional spectra in Figure 4 were collected using the longer delay times of 8, 20, and 30 μs, respectively. The spectra collected after a delay of 8 μs shows a small dip at the absorption maxima, which increased on going to longer, 20 and 30 μs, delays. This data demonstrates clearly that the phenomenon that causes the saturation dip occurs after the excitation laser pulse. Because no dip is present at the shortest delay time, all three multiple-photon processes may be eliminated as possible mechanisms for the saturation dips. The time delay in the appearance of the dip also precludes simple saturation of the optical transition as being the cause of the dip.

Amplified Spontaneous Emission

Other nonlinear effects considered included amplified spontaneous emission (ASE), superfluorescence, and stimulated emission.[22,23] Each of these processes can occur in rare-earth systems and are of particular interest in

the field of laser science. These processes can occur on meeting certain gain conditions and a sufficiently high density of excited states.[24] The mechanisms for the first two processes are illustrated in Figures 3b and 3c, where the horizontal dotted line in Figure 3b represents a radiative coupling between ions induced by prompt spontaneous radiation. Stimulated emission has the same general diagram as in Figure 3c, but with a coherent output. The dependence on excited-state density results in a nonlinear dependence and threshold condition for the excitation laser power. Because the excited-state density will most likely be met at an absorption maxima, especially in concentrated systems, any one of these processes could potentially explain the saturation dips. Significant line narrowing is usually observed for these processes. For example, the emission spectrum of $NdCl_3$ shows 20 sharp lines from 550 to 700 nm for excitation laser power less than 230 mW (at 12 K). Above the 230-mW threshold, only one spectrally narrowed line at 694.4 nm is observed, which is attributed to superfluorescence.[23] The intensity of this narrowed line also depended on the square of the laser power.

Saturation of excitation lines due to ASE, superfluorescence, or stimulated emission should result in changes in the relative intensity of fluorescence lines, with strong lines increasing at the expense of weaker lines, and some degree of fluorescent line narrowing. The $^5D_0 \rightarrow {}^7F_2$ transitions are the strongest *f-f* transitions in Eu_2O_3. The line at $\sim$612 nm dominates the $^5D_0 \rightarrow {}^7F_2$ spectrum and is the prime candidate for observing relative intensity changes or line narrowing. The fluorescence spectra of Eu_2O_3 at various excitation energies are shown in Figure 5. The figure shows that

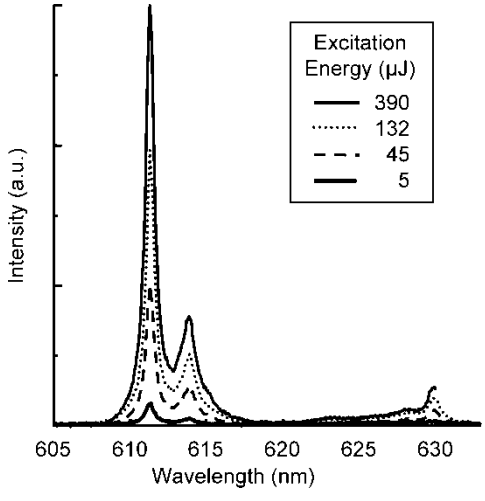

Figure 5. $^5D_0 \rightarrow {}^7F_2$ luminescence of cubic-phase Eu_2O_3 powder at various excitation densities (sample temperature $\sim$12 K, boxcar delay 1 μs and gate 150 μs).

there is no change in the relative intensity of the strong line at 612 nm compared with the two weaker $^5D_0 \rightarrow {}^7F_2$ lines at ~614 nm and ~630 nm as the laser power increases high enough to create the saturation dips. There is also no indication of narrowing of any of the $^5D_0 \rightarrow {}^7F_2$ lines. If ASE, superfluorescence, or stimulated emission were occurring, the strongest peak at 612 nm is expected to increase relative to the weaker peaks and to show narrowing. Because there is no change in the relative peak heights or linewidths as a function of excitation density, these nonlinear processes can be eliminated as possible mechanisms for the saturation effects.

Localized Heating

The integrated Eu^{3+} emission intensity of Eu_2O_3 is approximately 3% of the emission from optimally doped (~10%) Eu^{3+}:Y_2O_3.[8] The low luminescence quantum efficiency of Eu_2O_3 is attributed to nonradiative decay by concentration quenching and energy migration to quenching centers,[8] presumably resulting in the majority of absorbed radiation being converted to heat. Because the lifetime in Eu_2O_3 is temperature dependent,[8] a rapid temperature increase due to laser absorption might cause a decrease in the luminescence signal. The effects of localized heating were investigated because the largest amounts of heat would be produced at absorption maxima, which could lead to the observed saturation dips. Figure 6 shows a plot of the $^5D_0$ decay time versus temperature for Eu_2O_3. Between 12 K to 80 K, the fluorescence lifetime decreases significantly, but the decrease levels off above

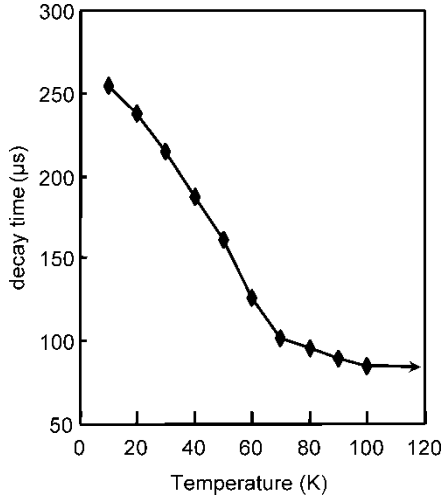

Figure 6. Plot of luminescence decay time versus temperature. Decay times were estimated using a fit to a single exponential function. The line is only a guide to the eye.

80 K. This plot is consistent with results by Buijs et al., in which the fluorescence lifetime did not change above 90 K.[8] If the saturation dip results from localized laser heating, then it should not be present at temperatures above 90 K because excess heat will not affect the fluorescence decay time. The temperature dependence study in Figure 7 shows that the saturation dip persists in the excitation spectra up to temperatures of at least 160 K. Localized heating is thus ruled out as the cause of the saturation effects. Additionally, the saturation dips were more easily produced in the crystal sample compared with the powder and nanocrystalline samples. A crystal should dissipate heat much better than a powder sample and therefore be more difficult to produce the saturation dips if the cause was localized heating. Examples of Eu_2O_3 excitation spectra using the crystal sample are presented in Figure 8. This example shows that the saturation effect occurs for the $^7F_0 \rightarrow {}^5D_1$ transition and also illustrates the potential use of the narrow dips to identify overlapping peaks, for example, three dips in the band at 528.4 nm, similar to Doppler-free spectroscopy.

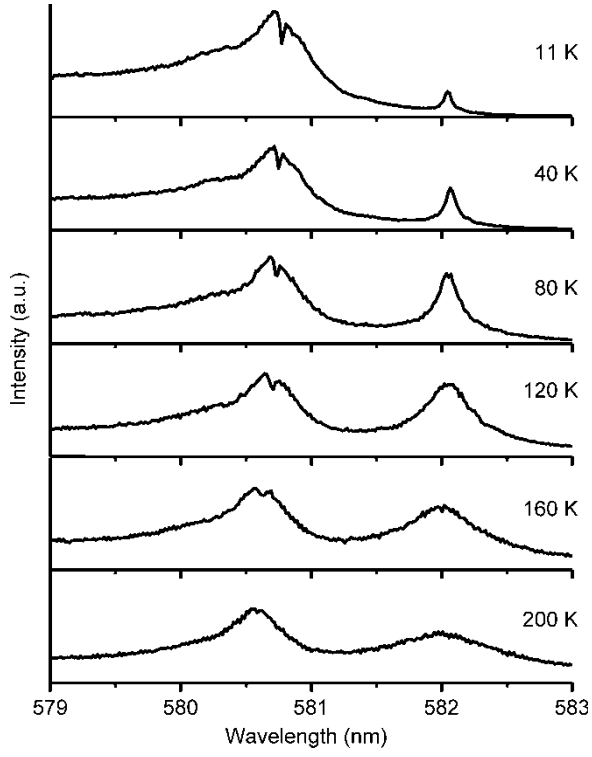

Figure 7. $^7F_0 \rightarrow {}^5D_0$ excitation spectra of cubic-phase Eu_2O_3 powder versus temperature.

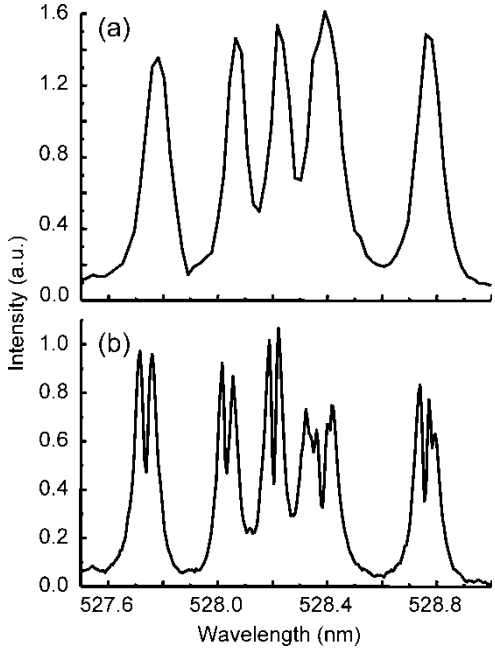

Figure 8. $^7F_0 \rightarrow {}^5D_1$ excitation spectra of monoclinic-phase Eu_2O_3 crystal. (a) Low laser excitation intensity and (b) high laser excitation intensity. The monoclinic phase has three crystallographic sites so a total of nine lines are possible in this spectral range.

Upconversion by Energy Transfer

The absorption spectrum of Eu_2O_3 consists of sharp lines due to intraconfigurational $4f^6$ transitions between 17,000 and 30,000 cm^{-1}, charge transfer bands at 43,500 cm^{-1} (230 nm) and 36,400 cm^{-1} (275 nm),[25] and broad band absorption due to $4f^6$ to $4f^5$5d transitions at energies above 40,000 cm^{-1}.[4] The emission spectrum consists of sharp lines due to transitions from the $^5D_0$ level to the lower ^7F_J levels. Emission from higher-energy excited states, such as $^5D_1$ and $^5D_2$, does not occur due to rapid cross-relaxation to the $^5D_0$ level.[26,27] Upconversion is a cross-relaxation process involving two excited ions that occurs for appropriate energy levels at a high excited-state density. The process is shown schematically in Figure 2d, where the solid arrows represent excitation of two nearby ions and the dashed arrows represent a nonradiative transfer of energy from one ion to the other. Energy level diagrams for cubic and monoclinic Eu_2O_3 are given in Refs. 8, 25, and 27. The energies are such that the lowest charge transfer band is sufficiently low to serve as the terminal level for the upconversion process (assuming that the charge transfer band of the monoclinic structure is similar to the cubic phase). The upconversion occurs only in the center of the inhomogeneously

broadened line because this is where the concentration of excited Eu^{3+} ions will be high enough for energy transfer to occur before the excited states are depopulated. The process is not expected to occur in the wings of a spectral line because an excited Eu^{3+} ion in a highly perturbed crystallographic site is not likely to be sufficiently close to another excited Eu^{3+} ion to transfer energy.

The upconversion causes a significant reduction in quantum efficiency at high excited-state densities achievable only at absorbance maxima.[28] The luminescence decay transient of Eu_2O_3 is initially nonexponential and becomes exponential after long times, which is characteristic of three-dimensional diffusion-limited energy migration. This makes it difficult to quantify the excitation density at which upconversion begins to influence luminescence decay. However, examination of luminescence decay at various excitation densities does support the occurrence of upconversion. The data presented in Figure 9 shows normalized luminescence decay curves taken at various excitation energies. The decay time shortens and becomes increasingly nonlinear as the excitation energy increases, which is consistent with the appearance of the additional intensity-dependent decay pathway provided by upconversion.

The process of upconversion by energy transfer has been documented for many concentrated lanthanide systems. Two examples, which provide good comparisons to Eu_2O_3, are $TbPO_4$ and TbF_3.[17,29] In both of the Tb materials, the occurrence of upconversion was verified by the observation of anti-Stokes luminescence, which is not observed in Eu_2O_3. In $TbPO_4$, a

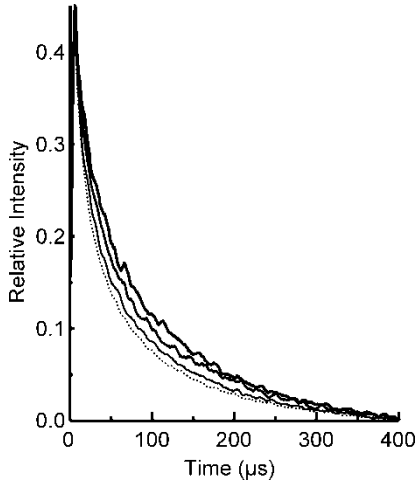

Figure 9. Normalized luminescence decay curves of cubic-phase Eu_2O_3 exciting $^5D_1$ and monitoring $^5D_0 \rightarrow {}^7F_2$ luminescence at 612 nm. Laser energies were 50, 80, 120, and 160 μJ for the curves from top to bottom, respectively.

nonexponential fluorescence decay was attributed to upconversion by energy transfer.[17] TbF_3 is particularly relevant, because like Eu_2O_3, saturation dips appear in the center of the excitation peaks.[29] These saturation dips were attributed to saturation of the optical transition in addition to intensity-dependent nonradiative pathways. The delayed appearance of the saturation dips in Eu_2O_3 (see Fig. 4) of the order several microseconds indicates that the intensity-dependent nonradiative mechanism predominates compared with optical saturation.

PHASE, PARTICLE SIZE, AND TRANSITION DEPENDENCE

The saturation dips were first recorded in excitation spectra of monoclinic-phase Eu_2O_3 nanoparticles. Experiments on a number of different samples show that the saturation effect is general for cubic and monoclinic phase Eu_2O_3 as nanoparticles, micrometer-sized powder, and crystals. The saturation dips were easiest to generate in the crystal sample. There was some difficulty maintaining a consistent laser focus with the powders as they were susceptible to ablation or settling at the laser focus, even though they were tightly packed into the sample holder. We were not able to make a quantitative comparison between different particle sizes due to this difficulty in obtaining a consistent and reproducible focus with the powder samples. The smallest particle size that we investigated was monoclinic phase with an average diameter of approximately 10 nm. The dips were not observed clearly, but we could confirm the saturation effect by the shortening of the luminescence transient as a function of excitation density, similar to the data shown in Figure 9.

The saturation dips were observed in both $^7F_0 \rightarrow {}^5D_0$ and $^7F_0 \rightarrow {}^5D_1$ spectra and in a $^7F_1 \rightarrow {}^5D_1$ transition at 534 nm at 80 K. In general, the dips appeared more pronounced in $^7F_0 \rightarrow {}^5D_1$ spectra, but a quantitative comparison between different transitions was not attempted. The difference is assumed to be due to the stronger intrinsic strength of the $^7F_0 \rightarrow {}^5D_1$ transitions rather than an energy level dependence in the upconversion process because the terminal level is a broad band. The observation of the dips for both the $^7F_0 \rightarrow {}^5D_1$ transitions and the intrinsically weaker $^7F_0 \rightarrow {}^5D_0$ line also indicates that simple saturation of the absorption transition is unlikely to be the cause of the dips, although some saturation is expected at some excitation energy.

CONCLUSIONS

We report nonlinear luminescence quenching that results in narrow saturation dips in the center of excitation spectral lines of Eu_2O_3. Of the several possible mechanisms that we investigated, only upconversion by energy

transfer is consistent with all of the spectroscopic data. Although energy migration and luminescent properties of europium-containing compounds are well studied,[9,30–35] most previous studies have not needed to consider contributions from excited-state interactions. Even in studies of Eu_2O_3, nonlinear luminescence quenching was not observed directly.[1,8,36,37] The only reports of nonlinear luminescence quenching we found for europium-containing compounds were europium-doped television phosphors, such as Eu^{3+}:Y_2O_3 and Eu^{3+}:Y_2O_2S. In these applications, the high excitation densities produced in cathode ray tubes can lead to nonlinear luminescence quenching by upconversion, which lowers the quantum efficiency.[20,38] The lack of reports of nonlinear luminescence quenching in concentrated europium systems is probably due to several reasons. First, the excitation density used in spectroscopic studies is much less than that achievable from cathode-ray excitation. Second, spectroscopy of concentrated europium compounds is generally done using powders, which have increased scattering of the excitation beam and, as we found, can be problematic in maintaining a steady laser focus compared with crystals. Finally, in order for upconversion to have a noticeable effect, the rate of energy transfer must be fast enough to bring excited ions together before they decay. The energy transfer rate in most europium compounds is not fast enough for this to occur, particularly at low temperatures where energy transfer is frozen in many cases.[3] The energy transfer rate in Eu_2O_3 is more rapid than other europium compounds, even at very low temperature.[3] So we predict that upconversion by energy transfer will be easier to produce in Eu_2O_3 than in other known europium compounds and is the most likely explanation for the saturation effects we observe. As a practical note, the narrow saturation dips are quite useful for determining the position of overlapping spectral lines, as seen in Figure 8.

ACKNOWLEDGMENT

This work was funded by the National Science Foundation under grant DMR-9871864.

REFERENCES

1. Sheng, K. C.; Korenowski, G. M. Laser-induced optical-emission studies of Eu^{3+} sites in polycrystalline powders of monoclinic and body-centered cubic Eu_2O_3. *J. Phys. Chem.* **1988**, *92* (1), 50–56.
2. Mochizuki, S.; Nakanishi, T.; Suzuki, Y.; Ishi, K. Reversible photoinduced spectral change in Eu_2O_3 at room temperature. *Appl. Phys. Lett.* **2001**, *79* (23), 3785–3787.
3. Blasse, G. Luminescence of inorganic solids — from isolated centers to concentrated systems. *Prog. Solid State Chem.* **1988**, *18* (2), 79–171.

4. Jüstel, T.; Nikol, H.; Ronda, C. New developments in the field of luminescent materials for lighting and displays. *Angew. Chem. Int. Ed.* **1998**, *37* (22), 3084–3103.
5. Kuriki, K.; Koike, Y.; Okamoto, Y. Plastic optical fiber lasers and amplifiers containing lanthanide complexes. *Chem. Rev.* **2002**, *102* (6), 2347–2356.
6. Klimov, V. I.; Mikhailovsky, A. A.; Xu, S.; Malko, A.; Hollingsworth, J. A.; Leatherdale, C. A.; Eisler, H. J.; Bawendi, M. G. Optical gain and stimulated emission in nanocrystal quantum dots. *Science* **2000**, *290* (5490), 314–317.
7. Nanda, J.; Ivanov, S. A.; Htoon, H.; Bezel, I.; Piryatinski, A.; Tretiak, S.; Klimov, V. I. Absorption cross sections and auger recombination lifetimes in inverted core/shell nanocrystals: implications for lasing performance. *J. Appl. Phys.* **2006**, *99* (3), 034309.
8. Buijs, M.; Meyerink, A.; Blasse, G. Energy transfer between Eu^{3+} ions in a lattice with 2 different crystallographic sites — Y_2O_3:Eu^{3+}, Gd_2O_3:Eu^{3+}, and Eu_2O_3. *J. Lumin.* **1987**, *37* (1), 9–20.
9. Buijs, M.; Blasse, G. One-dimensional and 3-dimensional energy migration in dimorphic EuP_3O_9. *J. Lumin.* **1988**, *39* (6), 323–334.
10. Tissue, B. M.; Bihari, B. Lanthanide luminescence as a probe of nanocrystalline materials. *J. Fluor.* **1998**, *8* (4), 289–294.
11. Plakhotnik, T.; Nonn, T.; Palm, V. Spectroscopy of vibronic transitions in single molecules. *Chem. Phys. Lett.* **2002**, *357* (5–6), 397–402.
12. Singh, S. K.; McCombe, B. D.; Kono, J.; Allen, S. J., Jr; Lo, I.; Mitchel, W. C.; Stutz, C. E. Saturation spectroscopy and electronic-state lifetimes in a magnetic field in $InAs/Al_xGa_{1-x}Sb$ single quantum wells. *Phys. Rev. B* **1998**, *58* (11), 7286–7291.
13. Eilers, H.; Tissue, B. M. Laser spectroscopy of nanocrystalline Eu_2O_3 and Eu^{3+}:Y_2O_3. *Chem. Phys. Lett.* **1996**, *251* (1–2), 74–78.
14. Adachi, G.; Imanaka, N. The binary rare earth oxides. *Chem. Rev.* **1998**, *98* (4), 1479–1514.
15. McPherson, R. Formation of metastable monoclinic rare earth sesquioxides from the melt. *J. Mater. Sci.* **1983**, *18* (5), 1341–1345.
16. Eilers, H.; Tissue, B. M. Synthesis of nanophase ZnO, Eu_2O_3, and ZrO_2 by gas-phase condensation with cw-CO_2 laser-heating. *Mater. Lett.* **1995**, *24*, 261–265.
17. Diggle, P. C.; Gehring, K. A.; Macfarlane, R. M. Exciton-exciton annihilation in $TbPO_4$. *Solid State Commun.* **1976**, *18* (3), 391–394.
18. Downer, M. C. The puzzle of 2-photon rare-earth spectra in solids. In *Laser Spectroscopy of Solids II*; Yen, W. M., (ed.); Springer-Verlag: Berlin, 1989, pp. 29–75.
19. Auzel, F. Upconversion and anti-stokes processes with f and d ions in solids. *Chem. Rev.* **2004**, *104* (1), 139–173.
20. Klaassen, D. B. M.; van Rijn, T. G. M.; Vink, A. T. A universal description of the luminescence saturation behavior per phosphor. *J. Electrochem. Soc.* **1989**, *136* (9), 2732–2736.
21. Hunt, R. B.; Pappalardo, R. G. Fast excited-state relaxation of Eu-Eu pairs in commercial Y_2O_3-Eu^{3+} phosphors. *J. Lumin.* **1985**, *34* (3), 133–146.
22. Rai, J.; Bowden, C. M. Quantum-statistical analysis of superfluorescence and amplified spontaneous emission in dense media. *Phys. Rev. A* **1992**, *46* (3), 1522–1529.
23. Yin, M.; Krupa, J. C. Superfluorescence from $NdCl_3$. *Chem. Phys. Lett.* **1999**, *314* (1–2), 27–30.
24. Siegman, A. E. *Lasers*; University Science Books: Mill Valley, CA, 1986; pp. 547–550.

25. Wakefield, G.; Keron, H. A.; Dobson, P. J.; Hutchison, J. L. Synthesis and properties of sub-50-nm europium oxide nanoparticles. *J. Coll. Interface Sci.* **1999**, *215* (1), 179–182.
26. Blasse, G.; Grabmaier, B. C. *Luminescent Materials*; Springer-Verlag: Berlin, 1994.
27. Bihari, B.; Eilers, H.; Tissue, B. M. Spectra and dynamics of monoclinic Eu_2O_3 and Eu^{3+}:Y_2O_3 nanocrystals. *J. Lumin.* **1997**, *75* (1), 1–10.
28. Cone, R. L.; Meltzer, R. S. Ion-ion interactions and exciton effects in rare earth insulators. In *Spectroscopy of Solids Containing Rare Earth Ions*; Kaplyanskii, A. A., and MacFarlane, R. M., (eds.); Elsevier: North-Holland, 1987, p. 481.
29. Joubert, M. F.; Jacquier, B.; Moncorge, R. Exciton-exciton annihilation and saturation effect in TbF_3. *Phys. Rev. B* **1983**, *28* (7), 3725–3732.
30. Berdowski, P. A. M.; Blasse, G. Luminescence and energy migration in a two-dimensional system — $NaEuTiO_4$. *J. Lumin.* **1984**, *29*, 243–260.
31. Berdowski, P. A. M.; Van Herk, J.; Blasse, G. Energy migration in a quasi-2-dimensional system — EuOCl. *J. Lumin.* **1985**, *34* (1–2), 9–18.
32. Blasse, G.; Dirksen, G. J.; Van Vliet, J. P. M. The luminescence of europium nitrate hexahydrate, $Eu(NO_3)_3 \cdot 6H_2O$. *Inorg. Chim. Acta* **1988**, *142*, 165–168.
33. Blasse, G.; Van Keulen, J.; Brixner, L. H. A study of the photoluminescence of Eu_3REO_8. *J. Lumin.* **1986**, *35*, 183–188.
34. Brittain, H. G.; Meyer, G. Cryogenic luminescence studies of Eu^{3+} in $LiEuCl_4$. *J. Solid State Chem.* **1985**, *59* (2), 183–189.
35. Kellendonk, F.; Blasse, G. Luminescence and energy-transfer in $EuAl_3B_4O_{12}$. *J. Chem. Phys.* **1981**, *75* (2), 561–571.
36. Dexpert-Ghys, J.; Faucher, M.; Caro, P. Site-selective excitation, crystal-field analysis, and energy-transfer in europium-doped monoclinic gadolinium sesquioxide — a test of the electrostatic model. *Phys. Rev. B* **1981**, *23*, 607–617.
37. Brittain, H. G.; Perry, D. L. Luminescence studies of lanthanide oxides. 1. Thermal and hydration effects on the metal-ion site symmetry in europium oxide catalysts. *J. Catal.* **1982**, *77* (1), 94–103.
38. Blasse, G. On the Eu^{3+} fluorescence of mixed metal oxides. IV. The photoluminescent efficiency of Eu^{3+}-activated oxides. *J. Chem. Phys.* **1966**, *45* (7), 2356–2360.